DMD Fast Forward. Published on June 14, 2019 as DOI: 10.1124/dmd.119.087148
This article has not been copyedited and formatted. The final version may differ from this version.

Title:

The enhancement of subcutaneous first-pass metabolism causes non-linear pharmacokinetics of TAK-448 after a single subcutaneous administration to rats

Authors:

Yuu Moriya, Akifumi Kogame, Yoshihiko Tagawa, Akio Morohashi, Takahiro Kondo, Satoru Asahi, Leslie Z. Benet.

Affiliations:

Drug Metabolism and Pharmacokinetics Research Laboratories, Pharmaceutical Research Division, Takeda Pharmaceutical Company Limited, Kanagawa, Japan (Y.M., A.K., Y.T., A.M., S.A.)

Analytical Development, Pharmaceutical Sciences, Takeda Pharmaceutical Company Limited, Osaka, Japan (T.K.)

University of California San Francisco, Department of Bioengineering and Therapeutic Sciences, Schools of Pharmacy and Medicine, San Francisco, CA, USA (L.Z.B)

Current affiliations:

Axcelead Drug Discovery Partners, Inc. (A.K., Y.T., S.A.)

Nemoto Science. Co., Ltd. (A.M.)

DMD Fast Forward. Published on June 14, 2019 as DOI: 10.1124/dmd.119.087148
This article has not been copyedited and formatted. The final version may differ from this version.

Running Title Page

Running Title:

Non-linear pharmacokinetics of TAK-448 in rats

Corresponding Author:

Name: Yuu Moriya, Ph. D.

Address: 26-1, Muraoka-Higashi 2-chome, Fujisawa, Kanagawa, Japan. 251-8555

E-mail: yuu.moriya@takeda.com

Phone: +81-466-32-1484

Fax: +81-466-29-4436

Text pages: 36

Number of tables: 3

Number of figures: 8

Number of references: 29

Abstract (words): 193

Introduction (words): 730

DMD Fast Forward. Published on June 14, 2019 as DOI: 10.1124/dmd.119.087148
This article has not been copyedited and formatted. The final version may differ from this version.

Discussion (words): 1437

List of Nonstandard abbreviations:

AEBSF, 4-(2-Aminoethyl) benzenesulfonyl fluoride; AUC, area under the plasma concentration-time curve; AUMC, area under the moment curve; BA, bioavailability; C_0, concentration at time 0; C_{5min}, concentration at 5 min after administration; CL_{tot}, total clearance; C_{max}, maximum concentration; DMAA, *N*, *N*-Dimethylacetamide; E-64, [(2S,3S)- 3- Carboxyoxirane- 2- carbonyl]- L- leucine (4- guanidinobutyl) amide; EDTA, ethylenediaminetetraacetic acid; GLP-1, glucagon-like peptide-1; GnRH, gonadotropin releasing hormone; GPR54, G-protein-coupled receptor 54; HPLC, high-performance liquid chromatography; IS, internal standard; IV, intravenous; LC-MS/MS, liquid chromatography tandem mass spectrometry; LSC, liquid scintillation counter; MAT, mean absorption time; $MLT_{ab\ site}$, mean time of loss from the absorption site; MRT, mean residence time; PBS, phosphate buffered saline; S.D., standard deviation; SC, subcutaneous; SD, Sprague-Dawley; SRM, selected reaction monitoring; $t_{1/2}$, half-life; T_{max}, time to reach C_{max}; $V_{d,ss}$, volume of distribution at steady-state

DMD Fast Forward. Published on June 14, 2019 as DOI: 10.1124/dmd.119.087148
This article has not been copyedited and formatted. The final version may differ from this version.

Abstract

TAK-448 (RVT-602), a kisspeptin analog, has been developed as a therapeutic agent for prostate cancer. The purpose of the present study is to clarify the mechanism of the less than dose-proportional non-linear pharmacokinetics of TAK-448 after subcutaneous (SC) administration to rats. Plasma pharmacokinetics of TAK-448 and radiolabeled TAK-448 ([^{14}C]TAK-448) were examined after SC and intravenous (IV) administration to rats. [^{14}C]TAK-448 was also subcutaneously injected together with protease inhibitors. The effects of the protease inhibitors on the *in vitro* metabolism of [^{14}C]TAK-448 were investigated using rat skin homogenates. In an dose ascending study, less than dose-proportional non-linear pharmacokinetics were observed after SC administration with limited absorption of TAK-448 at the highest dose level contrary to the linear pharmacokinetics following IV dosing, indicating an enhancement of SC metabolism with dose escalation. The systemic absorption of unchanged TAK-448 recovered when protease inhibitors were subcutaneously co-administered, suggested the involvement of SC proteases in the first-pass metabolism. An *in vitro* metabolism study suggests that serine protease could be responsible for the SC metabolism of TAK-448. A dose-dependent enhancement of first-pass metabolism appears to contribute to the less than dose-proportional non-linear pharmacokinetics of TAK-448

after SC administrations to rats.

DMD Fast Forward. Published on June 14, 2019 as DOI: 10.1124/dmd.119.087148
This article has not been copyedited and formatted. The final version may differ from this version.

Introduction

For many years prostate cancer has been treated by bilateral orchiectomy to eliminate testosterone production and by the administration of gonadotropin releasing hormone (GnRH) agonists. Continuous administration of GnRH agonists suppresses testosterone secretion by the down-regulation of gonadotropin secretion from the pituitary gland (Steinberg, 2009).

Kisspeptin was isolated from human placenta as a ligand of the human G-protein–coupled receptor OT7T175/GPR54 (Kotani et al., 2001; Muir et al., 2001; Ohtaki et al., 2001). Although kisspeptin was originally considered to be a metastasis suppressing peptide (Hori et al., 2001; Ohtaki et al., 2001; Stafford et al., 2002), it has been shown in mammals that kisspeptin has a pivotal role in the regulation of hypothalamic-pituitary-gonadal function. Deletions and mutations in GPR54 were also identified in patients with hypogonadotropic hypogonadism in the clinic (de Roux et al., 2003; Funes et al., 2003; Seminara et al., 2003). Administration of exogenous kisspeptin (45-54), the C-terminal 10 amino acid residue peptide of kisspeptin, induces gonadotropin secretion in the mouse, rat, monkey, and sheep, as well as in humans (Matsui et al., 2004).

TAK-448 (RVT-602) is a peptide analog of kisspeptin chemically synthesized by Takeda

Pharmaceutical Company Limited. *In vitro* and *in vivo* pharmacological studies have indicated that TAK-448 is a potent agonist of the kisspeptin receptor and continuous administration of TAK-448 rapidly reduced testosterone levels in rats (Matsui et al., 2012). The compound is being developed as a treatment for prostate cancer.

With the rapid advances in recombinant gene technology, biologically active peptide drugs have become widely prevalent such as the GLP-1 analog liraglutide, erythropoietin, interferon analogs, and GnRH analogs such as leuprolide (Brogden and Heel, 1987; Okada et al., 1988; Ogawa et al., 1989; Okada et al., 1994; Periti et al., 2002; Hadziyannis and Papatheodoridis, 2003; Elliott et al., 2008; Croom and McCormack, 2009). Since these peptide drugs would be orally inactive, they are generally administered via the parenteral route. We previously reported the disposition of TAK-448 after single subcutaneous (SC) and intravenous (IV) administration to rats and dogs with radiolabeled TAK-448 ([^{14}C]TAK-448) (Moriya et al., 2018). That study revealed that the dosed radioactivity was rapidly and almost completely absorbed after SC administration at pharmacologically effective doses and an appreciable amount of TAK-448 together with a hydrolyzed metabolite, M-I, were detected in the plasma of rats and dogs. In dogs, bioavailability (BA) of TAK-448 was 92.4% after SC administration. This value is comparable to the 96.8% ratio (SC/IV) for total

radioactivity at a dose of 1 mg/kg, suggesting that the subcutaneously dosed TAK-448 was almost completely absorbed in the unchanged form in dogs and the effect of first-pass metabolism at SC was minimal. On the other hand, although the radioactivity ratio of 94.1% for SC/IV was also comparable in rats, the BA of TAK-448 was much lower with a value of 66.3% in rats. This result suggests that TAK-448 underwent SC first-pass metabolism in rats. As described above, since TAK-448 is a synthetic peptide analog, some peptidases or proteases could be involved in the SC metabolism of TAK-448. Metabolic enzymes have been reported to be expressed in rat skin (Oesch et al., 2007), however, drug metabolism in skin is poorly understood compared with that in the primary drug metabolizing tissues.

The present study revealed that TAK-448 exhibited marked non-linear pharmacokinetics with less than dose-proportional increases of AUC at the doses of 0.1, 1 and 10 mg/kg after SC administration to rats, although the linear pharmacokinetics was observed after SC administration to dogs and monkeys (Supplemental Table 1 and 2). Particularly in the dose range from 1 to 10 mg/kg, the AUC was decreased even though the dose increased. The results of a pharmacokinetic study after IV administration to rats showed clear linearity over the same dose range, suggesting that SC metabolism may be a critical factor for the non-linearity of TAK-448 in rats. It is essential to examine the

mechanism of the non-linearity in pre-clinical studies; otherwise it might be difficult to estimate the effective concentration level from the results of early clinical trials. In the present study we investigated the mechanism for the less than dose-proportional non-linear pharmacokinetics involved in the first-pass metabolism of TAK-448 after SC administration to rats. The effects of protease inhibitors on the absorption of TAK-448 and the *in vitro* metabolism of TAK-448 in rat skin homogenates were also examined to clarify the properties of the SC metabolism in rats.

Materials and Methods

Materials

TAK-448, M-I and a structurally related internal standard were synthesized by Takeda Pharmaceutical Company Limited (Osaka, Japan). [^{14}C]TAK-448 was synthesized by GE Healthcare UK, Ltd. (Little Chalfont, Buckinghamshire, UK) and purified by Nemoto Science Co., Ltd. (Tokyo, Japan) with a specific activity of 5.72 – 6.59 MBq/mg. The chemical structures of [^{14}C]TAK-448, its M-I metabolite, and the internal standard T-1532583, with only one amino acid substitution with TAK-448 from Hyp to D-Trp, are shown in Figure 1. The radiochemical purity of [^{14}C]TAK-448, as verified by high-performance liquid chromatography (HPLC) equipped with an on-line liquid scintillation counter (LSC) detector, was more than 96.7%. A protease inhibitor cocktail for general use was purchased from Sigma-Aldrich Japan (Tokyo, Japan). 4-(2-Aminoethyl) benzenesulfonyl fluoride hydrochloride (AEBSF), Bestatin, Leupeptin Hemisulfate Monohydrate and Aprotinin from Bovine Lung were purchased from Wako Pure Chemical Industries (Osaka, Japan). EDTA·Na and [(2S,3S)- 3-Carboxyoxirane- 2- carbonyl]- L- leucine (4- guanidinobutyl) amide hemihydrate (E-64) were purchased from Dojindo Laboratories (Kumamoto, Japan) and the Peptide Institute, Inc. (Osaka, Japan), respectively. All other chemicals and reagents were

purchased from commercial sources.

Animals

Male Sprague-Dawley (SD) rats were purchased from Charles River Laboratories Japan, Inc. (Kanagawa, Japan). Animals were fed laboratory chow (CR-LPF from Oriental Yeast Co., Ltd., Tokyo, Japan), had free access to water, and were housed in temperature- and humidity-controlled rooms with 12 h light and dark cycles. Animal studies were conducted in accordance with the "Guideline for the Care and Use of Laboratory Animals in the Pharmaceutical Research Division, Takeda Pharmaceutical Company Limited", and were approved by the Ethical Committee for animal experiments for our division.

***In vivo* study**

TAK-448 and [^{14}C]TAK-448 were dissolved in *N*, *N*-Dimethylacetamide (DMAA)/5% glucose solution (1:9, v/v) for single SC and IV administration to rats. For single SC administration, the dosing solution and/or protease inhibitor cocktail were injected dorsally to non-fasted male rats. For single IV administration, the dosing solution was injected into the femoral veins of non-fasted male rats.

After SC and IV administrations of TAK-448 or [^{14}C]TAK-448 to rats, blood was collected from the tail veins at the designated time points and centrifuged at approximately 8000 × g at 4°C for 3 minutes to obtain plasma; the total radioactivity or the concentration of TAK-448 was measured as described below.

For the preparation of the injection formulation for the protease inhibitor, a bottle of protease inhibitor cocktail (Sigma-Aldrich Japan, Tokyo, Japan) was added with 2 mL of 10 mM PBS. To examine the effect of the SC co-administration of the protease inhibitor cocktail on the pharmacokinetics of [^{14}C]TAK-448 after SC dosing, the dosing solution of [^{14}C]TAK-448 and the protease inhibitor cocktail solution were mixed in a volume ratio of 3:2 to achieve final concentrations of [^{14}C]TAK-448 from 1 to 10 mg/mL/kg, and the concentrations of the protease inhibitors were as follows: 40 mM AEBSF, 20 mM EDTA, 2.6 mM bestatin, 0.28 mM E-64, 0.02 mM leupeptin, and 0.006 mM aprotinin. The effect of the SC dosing of the protease inhibitor cocktail on the pharmacokinetics of [^{14}C]TAK-448 after IV administration to rats was also examined. Protease inhibitor cocktail was dorsally injected and [^{14}C]TAK-448 was subsequently injected into the femoral vein of rats.

Preparation of skin homogenates

Male SD rat was sacrificed by exsanguination from the abdominal aorta under anesthesia with ether, and beagle dog and cynomolgus monkey were sacrificed by overdosing with sodium pentobarbital at an intravenous dose of about 50 mg/kg, followed by excision of about 25 cm^2 of the dorsal skin. Human skin (female, Caucasian, 22 cm^2) was obtained from a commercial source (KAC, Kyoto, Japan). Rat skin was collected just before preparation of the homogenates, and the others were stored in a freezer with a controlled range of –90 to –70°C until used. The following procedure was conducted under ice-chilled conditions. After trimming off excessive muscle and connective tissue the skin was finely minced and weighed. The minced skin was transferred into a flask and homogenized in 10 mM PBS to prepare a homogenate at a concentration of 10% (w/v). The homogenate was centrifuged at approximately 1,500 × g at 4°C for 10 minutes, and the middle layer was obtained as a skin homogenate. The skin homogenate was diluted with 10 mM PBS for measurement of protein concentrations, and the remaining homogenate was stored in a freezer with a controlled temperature range of –90 to –70°C and shielded from light until used. Protein concentrations were determined using an assay kit (Coomassie Plus Reagent) with bovine serum albumin as a standard.

***In vitro* metabolism of [^{14}C]TAK-448 in the skin homogenate**

1 mL of PBS containing 900 μg protein of the skin homogenate with or without protease inhibitors, and the homogenate containing 100 μg/mL of unlabeled TAK-448 were pre-incubated at 37°C for 5 minutes except for the samples for time 0 and for incubation at 4°C. The metabolism study was initiated by addition of 10 μL of [^{14}C]TAK-448 PBS solution (1 μg/mL at the final concentration) followed by incubation at 4 or 37°C for the designated times. After the incubation for the designated times, 1 mL of the stop solution (methanol/0.5% formic acid, 1000/1, v/v) was added to terminate the reaction. For the incubation time of 0 minute, a 1 mL aliquot of the stop solution was added to 1 mL of the skin homogenate mixture, followed by the addition of 10 μL of [^{14}C]TAK-448 under ice-chilled conditions. For inactivation of the metabolic enzymes, the rat skin homogenates were incubated in a hot water bath at 80°C for 15 minutes followed by storage at 4°C until used in the metabolism study. The protease inhibitor cocktail used in this study contained 6 mM AEBSF, 3 mM EDTA·Na, 390 μM bestatin, 43 μM E-64, 3 μM leupeptin and 0.9 μM aprotinin, and the effects of each component were examined.

LC-MS/MS analysis

Concentrations of TAK-448 in rat plasma were determined using liquid chromatography tandem mass spectrometry (LC-MS/MS) using the internal standard (IS), T-1532583. The LC system was an LC-20A system (Shimadzu Co., Kyoto, Japan), while the mass spectrometer was an API4000 system (Applied Biosystems/MDS Sciex, Foster City, CA, USA) equipped with an electrospray ionization source. The column used was an Inertsil ODS-3 (150 mm × 2.1 mm i.d., particle size 5 μm; GL Science, Tokyo, Japan). Column temperature was maintained at 40°C. Purified water/ acetic acid (500:1, v/v) as the mobile phase A and methanol/ acetic acid (500:1, v/v) as the mobile phase B were used with varying compositions at a flow rate of 0.2 mL/min. The HPLC gradient program was time (min)/ % of B (v/v): 0/15, 1/15, 4/70, 8.5/70, 8.6/15 and 15/15. The turbo ion spray interface was operated in the positive ion mode at an ionization voltage of 5500 V with a turbo gas heater at 550°C. Curtain gas, ion source gas 1, ion source gas 2, and collision gas were at 40 psi (276 kPa), 50 psi (345 kPa), 80 psi (552 kPa) and 10, respectively. Quantitation was performed by selected reaction monitoring (SRM). The mass transition was from m/z 613.5 to 511.0 for TAK-448 and from m/z 649.8 to 754.2 for the IS. The collision energy and dwell time for TAK-448 and the IS were 23 V and 17 V, and 0.15 s for each compound, respectively. The analytical data were processed with Analyst software, version 1.4.1 (Applied Biosystems/MDS Sciex).

DMD Fast Forward. Published on June 14, 2019 as DOI: 10.1124/dmd.119.087148
This article has not been copyedited and formatted. The final version may differ from this version.

Analytical methods for the ^{14}C samples

The radioactivity in the biological samples, organic solvent extract and the samples for HPLC was determined by LSC as reported previously (Tanayama et al., 1978; Kondo et al., 1995). The radioactivity in the plasma and organic solvent was directly counted in a toluene-phosphor mixture containing nonionic detergent. [^{14}C]TAK-448 and its metabolite in the plasma and the reaction mixture after the metabolism in the skin homogenates were analyzed by an HPLC equipped with an on-line LSC detector as reported previously (Moriya et al., 2018). The HPLC consisted of a Waters 2795 HPLC system (Waters Corp., Milford, MA, USA) with a Capcellpak C_{18} MG II column (250 mm × 4.6 mm i.d., particle size 5 μm; Shiseido Co. Ltd., Tokyo, Japan) for separation of TAK-448 and its related compounds. The column temperature was maintained at 40°C. 0.05 mol/L ammonium formate/ distilled water/ acetonitrile/ formic acid (10:80:10:0.05, by vol.) as the mobile phase A and 0.05 mol/L ammonium formate/ acetonitrile/ formic acid (10:90:0.05, by vol.) as the mobile phase B were used with varying compositions and the flow rate was 1.0 mL/min. The HPLC gradient program was time (min)/ % of B (v/v): 0/0, 10/0, 35/40, 40/90, 40.1/0 and 55/0. The radioactive materials in plasma were extracted with 5 volumes of the extracting solution

(methanol/ formic acid, 1000:1, v/v). After evaporation of the organic solvent under a nitrogen stream, the residue was dissolved in a small volume of mobile phase A. For samples obtained in the *in vitro* study, after the termination of the metabolic reaction, the samples were centrifuged at approximately 1500 × g at 10°C for 10 minutes to obtain the supernatants. The supernatants were evaporated to dryness under a nitrogen stream and the residues were dissolved in mobile phase A, followed by composition analysis. Radioactivity was monitored on-line by a Radiomatic 625TR (PerkinElmer. Inc. Waltham, MA, USA). Under these conditions, TAK-448 and M-I were eluted at about 30 and 7 min, respectively.

Data analysis

Concentrations of total radioactivity in the biological samples and those of the metabolite in the plasma were expressed as TAK-448 equivalent values. The data are reported as mean values or mean values ± standard deviation (S.D.). Metabolic profiles of the radioactivity in the rat plasma were determined using pooled samples from three animals. Maximum concentration (C_{max}), time to reach C_{max} (T_{max}) and C_{5min} were established directly from the plasma concentration data. Half-life ($t_{1/2}$), the area under the plasma concentration-time curve (AUC), area under the moment curve

(AUMC), volume of distribution at steady-state ($V_{d,ss}$) and total clearance (CL_{tot}) were calculated by non-compartmental methods in WinNonlin (Ver. 6.3, Pharsight Corp., Mountain View, CA, USA). Following IV bolus dosing AUMC/AUC is the mean residence time (MRT) in the systemic circulation. Frequently the mean absorption time (MAT) is calculated as the difference between AUMC/AUC following non-IV bolus administration (frequently oral, but here SC) and MRT. However, this difference is, in fact, the mean time of loss from the absorption site, which we have designated here as $MLT_{ab\ site}$, since both absorption from and degradation at the absorption site affect this parameter. The values for $t_{1/2}$ were calculated by the least-squares method and AUC and AUMC by the linear trapezoidal method.

The ratio of the concentration of TAK-448 in the skin homogenate after the reaction (Remaining % of initial) was calculated by the following equation:

$$\text{Remaining \% of initial} = Ct / C_0 \times 100$$

where Ct is the concentration of TAK-448 in the skin homogenate after the incubation at 4 or 37°C for designated time points, and C_0 is that at time 0.

Results

Non-linear pharmacokinetics of TAK-448 after a single subcutaneous administration to rats

The linearity in the plasma pharmacokinetics of TAK-448 was investigated after single SC and IV administration to rats (Figs. 2 and 3, Table 1). After SC administration of TAK-448 at a dose of 0.1 mg/kg, the concentration of TAK-448 reached the maximum of 90.0 ng/mL (C_{max}) at 0.5 h (T_{max}), and then the compound was rapidly eliminated with a half-life ($t_{1/2}$) of 0.5 h. The AUC was calculated to be 123 ng·h/mL at that dose. At the SC dose of 1 mg/kg, the C_{max} and AUC were increased at a less than dose proportional manner to 381.3 ng/mL and 804 ng·h/mL, respectively. However, when the dose was increased to 10 mg/kg, the C_{max} and AUC decreased to 284.6 ng/mL and 309 ng·h/mL, respectively. Although $t_{1/2}$ values were scarcely affected by the dose escalation, T_{max}, AUMC/AUC and $MLT_{ab\ site}$ were decreased at the highest SC dose. On the other hand, almost linear pharmacokinetics were observed after IV administration of TAK-448 over the dose range of 0.01 to 10 mg/kg (Table 1). The concentration at 5 min after administration (C_{5min}), the first sampling time, and the AUC showed almost dose-proportional increases as shown in Table 1. The $t_{1/2}$ and MRT were almost constant and the $t_{1/2}$ values were comparable with those observed after SC

administrations. The values of $V_{d,ss}$ and CL_{tot} were constant over the IV dose range of 0.01 to 10 mg/kg.

Non-linearity of the first-pass metabolism after a single subcutaneous administration of [^{14}C]TAK-448 to rats

The concentrations of total radioactivity, TAK-448 and M-I, a hydrolyzed metabolite, in the plasma of rats were investigated after SC and IV administration of [^{14}C]TAK-448 (Fig. 4 and Table 2). After SC administration, the increases in the C_{max} and AUC for total radioactivity were slightly less than dose-proportional; C_{max} was 1.124 and 6.361 μg/mL and AUC was 2.326 and 16.020 μg·h/mL at 1 and 10 mg/kg, respectively. On the other hand, ascending doses of [^{14}C]TAK-448 from 1 to 10 mg/kg showed noticeable decreases of C_{max} and AUC of TAK-448; C_{max} was 0.624 and 0.410 μg/mL, and AUC was 1.184 and 0.386 μg·h/mL at the SC doses of 1 and 10 mg/kg, respectively. Based on the AUCs, 50.9% and 2.4% of the total radioactivity were accounted for by TAK-448 after SC administration of [^{14}C]TAK-448 to rats at doses of 1 and 10 mg/kg, respectively. In contrast, C_{max} and AUC of M-I showed more than dose-proportional increases within the SC dose range of 1 and 10 mg/kg. Composition analysis of the rat plasma after IV administration of [^{14}C]TAK-448 at a dose of 1 mg/kg indicated that

TAK-448 was the major component accounting for 76.4% of the total radioactivity based on the AUCs.

Effect of the subcutaneous co-administration of the protease inhibitor cocktail on the pharmacokinetics of TAK-448

The influence of a subcutaneously co-administered protease inhibitor cocktail on the pharmacokinetics of the total radioactivity, TAK-448 and M-I in rats was examined after SC and IV administration of [^{14}C]TAK-448 (Fig. 5 and Table 3). The concentrations of the protease inhibitors were 40 mM AEBSF, 20 mM EDTA, 2.6 mM bestatin, 0.28 mM E-64, 0.02 mM leupeptin, and 0.006 mM aprotinin in the dosing formulation. After SC co-administration of [^{14}C]TAK-448 and the protease inhibitors to rats, in contrast to the results depicted in Fig. 4, C_{max} and AUC of TAK-448 were not decreased, but increased less than dose-proportionally while those of M-I increased dose-proportionally with the dose increase from 1 to 10 mg/kg. In addition, SC co-administration of the protease inhibitors increased the C_{max} and AUC of TAK-448 at the dose of 10 mg/kg compared to those without inhibitors, while those of M-I were less than those without protease inhibitors (Tables 2 and 3). On the other hand, the comparison of the pharmacokinetic parameters indicated that SC co-administration of

the protease inhibitors had little effect on the plasma concentration profiles for all the components after IV administration of [^{14}C]TAK-448 (Tables 2 and 3).

In vitro metabolism of [^{14}C]TAK-448 in rat skin homogenates

The time profiles for the degradation of [^{14}C]TAK-448 (1 μg/mL) in the skin homogenates prepared from rats were examined (Fig. 6). The spiked [^{14}C]TAK-448 was rapidly degraded in a time-dependent manner with a $t_{1/2}$ of 14.4 min at 37°C. To examine whether the degradation of TAK-448 was mediated by metabolic enzymes, the reaction was performed under ice-chilled conditions or was performed using a pre-heated homogenate at 80°C for 15 minutes (Fig. 7), under which condition the metabolic enzymes were reported to be inactivated (Sato et al., 2008). After incubation for 60 min with rat skin homogenate the residual ratio of TAK-448 was 91.2% and 98.2% for ice-chilled and pre-heated samples, respectively. The concentration-dependency of the metabolism was examined at the concentration of 100 μg/mL of TAK-448, and the residual ratio at the termination of the reaction was 3.6% (Fig. 7). In addition, the inhibitory effects of the protease inhibitor cocktail, also used in the *in vivo* study, and its ingredients on the metabolism of TAK-448 were investigated to determine the enzymes responsible for the SC metabolism of TAK-448 (Fig. 8). In

the presence of the protease inhibitor cocktail, the metabolism of TAK-448 was significantly inhibited; the residual ratio at 60 min after the initiation of the reaction was 76.5%. AEBSF and EDTA had also the inhibitory effects on the metabolism with the residual ratios of 71.7% and 16.7% at the termination of the reaction, respectively. The other components, bestatin, E-64, leupeptin and aprotinin had little effect.

Species differences in the metabolism of [^{14}C]TAK-448 with skin homogenates

Metabolism of [^{14}C]TAK-448 (1 μg/mL) in the skin homogenates were compared among rat, dog, monkey and human. After incubation for 60 min with the skin homogenates the residual ratio of TAK-448 was 5.5%, 14.8%, 14.4% and 45.6% in rat, dog, monkey and human, respectively.

Discussion

In the present study, we attempted to clarify the mechanism for the less than dose-proportional non-linear pharmacokinetics after single dose SC administration of TAK-448 to rats and ascertained that first-pass metabolism via proteases in the rat skin could be involved in the non-linearity.

Our previous pharmacokinetic study with [^{14}C]TAK-448 revealed that BA of TAK-448 was lower than F_{app} of total radioactivity after SC administration to rats, suggesting that TAK-448 underwent first-pass skin metabolism (Moriya et al., 2018). In the present study the markedly less than dose-proportional non-linear pharmacokinetics were observed after a single SC administration of TAK-448 to rats in the dose range from 0.1 to 10 mg/kg (Figs. 2 and 3, Table 1). AUC increased from 123 to 804 ng·h/mL after SC doses from 0.1 to 1 mg/kg. However, with the increase in SC dose from 1 to 10 mg/kg, AUC decreased to 309 ng·h/mL. In contrast to SC administration, the pharmacokinetics was almost linear after IV administration in the dose range from 0.01 to 10 mg/kg, suggesting that the non-linearity was specific to SC administration with dose-dependent enhancement of the pre-systemic clearance, and thus would not be caused by saturation of the plasma protein binding or induction of metabolizing enzymes. We previously reported the moderate and almost constant plasma protein

binding of TAK-448 in rats (Moriya et al., 2018). It would be also quite unlikely that the enzymes were induced after single dose. We attempted to clarify these nonlinear pharmacokinetic properties following SC administration by using [^{14}C]TAK-448 and a protease inhibitor cocktail.

The dose ascending study of [^{14}C]TAK-448 after single SC administration to rats suggested that the SC metabolism of TAK-448 could be markedly facilitated with the dose increase from 1 to 10 mg/kg (Fig. 4 and Table 2). Although AUC of TAK-448 decreased from 804 to 309 ng·h/mL after SC administration of unlabeled TAK-448 at the doses of 1 and 10 mg/kg, AUC of total radioactivity was increased from 2.326 to 16.020 μg·h/mL after SC administration of [^{14}C]TAK-448 in the same dose range, suggesting the influence of radiolabeled metabolites. The composition analysis showed that, based on AUC ratios, 50.9% and 2.4% of total radioactivity was accounted for by TAK-448 after SC administration of [^{14}C]TAK-448 at the doses of 1 and 10 mg/kg, respectively. On the other hand, the composition ratios of M-I, a hydrolyzed metabolite, increased from 30.6% to 84.5% in the same dose range. These results suggest that the SC metabolism of TAK-448 to M-I showed dose-dependent enhancement from 1 to 10 mg/kg.

The extent and the rate of the metabolism in skin have been reported to affect the

absorption of subcutaneously injected drugs and a lot of efforts have been made to increase the BA. BA of subcutaneously injected insulin was increased by the co-administration of collagen or by pretreatment with an ointment containing protease inhibitors in rats and humans, suggesting that the collagen or the protease inhibitors prevented insulin from degradation by the proteolytic enzymes in SC tissue (Hori et al., 1989; Takeyama et al., 1991). To further characterize the SC degradation of TAK-448 in rats, we examined the effects of SC co-administration of a protease inhibitor cocktail (Fig. 5 and Table 3). The SC co-administration had little effect on the pharmacokinetic parameters of total radioactivity after a single SC and IV dose of 1 mg/kg; however, it significantly increased the AUC of TAK-448, along with a reduction of M-I, at a SC dose of 10 mg/kg compared to that observed without the protease inhibitors (Tables 2 and 3). These results suggest that subcutaneous metabolism by proteases might contribute to the reduced absorption of TAK-448 at the high dose. It has been reported that most proteases are synthesized as inactive precursors (zymogens) and are usually converted to the active enzyme by proteolytic processing mediated either by other proteases or by autocatalysis (Neurath, 1999). It is possible that TAK-448 at high concentration could trigger the proteolytic cascade and activate the proteases responsible for the SC metabolism of TAK-448. A more detailed characterization of

the mechanism for the dose-dependent enhancement of the SC metabolism is required to understand the non-linearity observed for TAK-448. However, the present study highlights a previously under-emphasized aspect of calculating mean absorption times. In Table 1 we calculate the $MLT_{ab\ site}$ as the difference between AUMC/AUC following SC vs IV administration. This mean loss time parameter is the sum of the mean absorption time and mean degradation time at the absorption site. By apparently activating the enzymes at the absorption site we have markedly increased the rate of metabolism at the absorption site, thereby markedly decreasing the calculated $MLT_{ab\ site}$ for the 10 mg/kg dose, probably with little effect on the actual mean absorption time. That is, since so little of the dose is absorbed, the value for $MLT_{ab\ site}$ is predominantly a measure of the rapid increase in degradation rate.

In vitro studies were performed to characterize the degradation of TAK-448 in rat skin homogenate (Figs. 6 and 7), and the results suggest that TAK-448 was metabolized by proteases sensitive to serine protease inhibitors. When incubated with rat skin homogenate, [^{14}C]TAK-448 was degraded in a time-dependent manner with a $t_{1/2}$ of 14.4 minutes, and was temperature-dependent. Moreover there was no degradation of [^{14}C]TAK-448 when the metabolic enzymes were inactivated by pre-heat treatment. Time- and temperature-dependency suggest that the degradation of TAK-448 was

mediated by metabolic enzymes. However, concentration-dependency was not observed at least up to 100 μg/mL, indicating that the responsible enzyme has a low affinity for TAK-448. The metabolic enhancement was observed *in vivo* associated with enzyme activation, and there would be a limit to quantitative consideration because it would be difficult to assess the enzyme activation from the *in vitro* study. A sensitivity profile to specific protease inhibitors was examined to identify the class of protease responsible for the metabolism of TAK-448 in rat skin homogenate (Fig. 8). In the presence of a protease inhibitor cocktail the metabolism of TAK-448 was significantly inhibited with the remaining percentage of 76.5%. The protease inhibitor cocktail used in this metabolic study consisted of 6 mM AEBSF, 3 mM EDTA·Na, 390 μM bestatin, 43 μM E-64, 3 μM leupeptin and 0.9 μM aprotinin, and the inhibitory effects of each component were also investigated. Among the constituents of the protease inhibitor cocktail, AEBSF and EDTA inhibited the metabolism of TAK-448 in rat skin homogenate, and the remaining ratio of TAK-448 was 71.7% and 16.7% of the initial concentration, respectively. AEBSF and EDTA are known to be, respectively, an irreversible inhibitor of serine proteases and a reversible metalloprotease inhibitor. These results suggest that [^{14}C]TAK-448 would be metabolized by enzymes sensitive to the serine protease inhibitor. Some serine proteases, such as kallikrein, plasmin,

plasminogen activator and matrix metalloproteases, are reported to be expressed in skin (Lundwall and Brattsand, 2008; Toriseva and Kahari, 2009), and further studies will be required to identify which serine protease was involved in SC metabolism of TAK-448.

The non-clinical pharmacokinetic studies suggest that a high SC dose of TAK-448 could possibly lead to a limited exposure of this compound in the clinic. The non-linear pharmacokinetics in rats with less than dose proportionality was sensitive to protease inhibitors (Table 2 and 3). Although the mechanism is still unclear, the enhancement of protease activity would definitely be related to the non-linearity at high doses in rats. Even though the similar enhancement could occur, dogs and monkeys showed almost linear pharmacokinetics after SC administration of TAK-448 at up to 10 mg/kg (supplemental table 1 and 2), probably because the metabolic activities are lower in dogs and monkeys compared to rats as shown in our *in vitro* data. If it is true, we don't think the severe non-linear pharmacokinetics would be observed in human with the lowest metabolic activity *in vitro*. In addition, the low SC dose of TAK-448 showed moderate absorption with BA of more than 65% in rats (Moriya et al., 2018), suggesting that a slow-release formulation could be a reasonable approach to avoid unfavorable pharmacokinetics in the clinical development of TAK-448.

In conclusion, it was demonstrated that TAK-448 showed less than dose-proportional

non-linear pharmacokinetics with a reduction of AUC after SC administration in a dose range of 1 and 10 mg/kg to rats. Our results suggested that SC first-pass metabolism would be enhanced for the peptide predominantly metabolized by serine proteases. This is the first report of a dose-dependent enhancement of the SC metabolism of a drug. Our study showed the importance of characterization of enzymes involved in SC metabolism of peptide drugs, which leads to mitigation of the risk of low exposure of subcutaneously administered peptide drugs in clinical.

Authorship Contributions

Participated in research design: Moriya, Kogame, Tagawa, Benet

Conducted experiments: Moriya

Performed data analysis: Moriya, Kogame, Tagawa

Wrote or contributed to the writing of the manuscript: Moriya, Kogame, Tagawa, Morohashi, Kondo, Asahi, Benet

References

Brogden RN and Heel RC (1987) Human insulin. A review of its biological activity, pharmacokinetics and therapeutic use. *Drugs* **34:** 350-371.

Croom KF and McCormack PL (2009) Liraglutide: a review of its use in type 2 diabetes mellitus. *Drugs* **69:** 1985-2004.

de Roux N, Genin E, Carel JC, Matsuda F, Chaussain JL, and Milgrom E (2003) Hypogonadotropic hypogonadism due to loss of function of the KiSS1-derived peptide receptor GPR54. *Proc Natl Acad Sci U S A* **100:** 10972-10976.

Elliott S, Pham E, and Macdougall IC (2008) Erythropoietins: a common mechanism of action. *Exp Hematol* **36:** 1573-1584.

Funes S, Hedrick JA, Vassileva G, Markowitz L, Abbondanzo S, Golovko A, Yang S, Monsma FJ, and Gustafson EL (2003) The KiSS-1 receptor GPR54 is essential for the development of the murine reproductive system. *Biochem Biophys Res Commun* **312:** 1357-1363.

Hadziyannis SJ and Papatheodoridis GV (2003) Peginterferon-alpha2a (40 kDa) for chronic hepatitis C. *Expert Opin Pharmacother* **4:** 541-551.

Hori A, Honda S, Asada M, Ohtaki T, Oda K, Watanabe T, Shintani Y, Yamada T, Suenaga M, Kitada C, Onda H, Kurokawa T, Nishimura O, and Fujino M (2001) Metastin suppresses the motility and growth of CHO cells transfected with its receptor. *Biochem Biophys Res Commun* **286:** 958-963.

Hori R, Komada F, Iwakawa S, Seino Y, and Okumura K (1989) Enhanced bioavailability of subcutaneously injected insulin coadministered with collagen in rats and humans. *Pharm Res* **6:** 813-816.

Kondo T, Kurata Y, Yoshida K, and Yoshimura Y (1995) Disposition of DN-2327, a new anxiolytic, in rats, dogs, and monkeys. *Biol Pharm Bull* **18:** 330-336.

Kotani M, Detheux M, Vandenbogaerde A, Communi D, Vanderwinden JM, Le Poul E, Brezillon S, Tyldesley R, Suarez-Huerta N, Vandeput F, Blanpain C, Schiffmann SN, Vassart G, and Parmentier M (2001) The metastasis suppressor gene KiSS-1 encodes kisspeptins, the natural ligands of the orphan G protein-coupled receptor GPR54. *J Biol Chem* **276:** 34631-34636.

Lundwall A and Brattsand M (2008) Kallikrein-related peptidases. *Cell Mol Life Sci* **65:** 2019-2038.

Matsui H, Takatsu Y, Kumano S, Matsumoto H, and Ohtaki T (2004) Peripheral administration of metastin induces marked gonadotropin release and ovulation in the rat.

Biochem Biophys Res Commun **320:** 383-388.

Moriya Y, Kogame A, Tagawa Y, Morohashi A, Kondo T, and Asahi S (2018) Investigation of disposition for TAK-448, a synthetic peptide of kisspeptin analog, in rats and dogs using the radiolabeled TAK-448 suitable for pharmacokinetic study. *Xenobiotica***:** 1-7.

Muir AI, Chamberlain L, Elshourbagy NA, Michalovich D, Moore DJ, Calamari A, Szekeres PG, Sarau HM, Chambers JK, Murdock P, Steplewski K, Shabon U, Miller JE, Middleton SE, Darker JG, Larminie CG, Wilson S, Bergsma DJ, Emson P, Faull R, Philpott KL, and Harrison DC (2001) AXOR12, a novel human G protein-coupled receptor, activated by the peptide KiSS-1. *J Biol Chem* **276:** 28969-28975.

Neurath H (1999) Proteolytic enzymes, past and future. *Proc Natl Acad Sci U S A* **96:** 10962-10963.

Oesch F, Fabian E, Oesch-Bartlomowicz B, Werner C, and Landsiedel R (2007) Drug-metabolizing enzymes in the skin of man, rat, and pig. *Drug Metab Rev* **39:** 659-698.

Ogawa Y, Okada H, Heya T, and Shimamoto T (1989) Controlled release of LHRH agonist, leuprolide acetate, from microcapsules: serum drug level profiles and pharmacological effects in animals. *J Pharm Pharmacol* **41:** 439-444.

Ohtaki T, Shintani Y, Honda S, Matsumoto H, Hori A, Kanehashi K, Terao Y, Kumano S, Takatsu Y, Masuda Y, Ishibashi Y, Watanabe T, Asada M, Yamada T, Suenaga M, Kitada C, Usuki S, Kurokawa T, Onda H, Nishimura O, and Fujino M (2001) Metastasis suppressor gene KiSS-1 encodes peptide ligand of a G-protein-coupled receptor. *Nature* **411:** 613-617.

Okada H, Doken Y, Ogawa Y, and Toguchi H (1994) Preparation of three-month depot injectable microspheres of leuprorelin acetate using biodegradable polymers. *Pharm Res* **11:** 1143-1147.

Okada H, Heya T, Ogawa Y, and Shimamoto T (1988) One-month release injectable microcapsules of a luteinizing hormone-releasing hormone agonist (leuprolide acetate) for treating experimental endometriosis in rats. *J Pharmacol Exp Ther* **244:** 744-750.

Periti P, Mazzei T, and Mini E (2002) Clinical pharmacokinetics of depot leuprorelin. *Clin Pharmacokinet* **41:** 485-504.

Sato T, Mizuno K, and Ishii F (2008) In vitro metabolism study of edaravone in Wistar and hairless rat skin. *Biol Pharm Bull* **31:** 1150-1154.

Seminara SB, Messager S, Chatzidaki EE, Thresher RR, Acierno JS, Jr., Shagoury JK, Bo-Abbas Y, Kuohung W, Schwinof KM, Hendrick AG, Zahn D, Dixon J, Kaiser UB,

Slaugenhaupt SA, Gusella JF, O'Rahilly S, Carlton MB, Crowley WF, Jr., Aparicio SA, and Colledge WH (2003) The GPR54 gene as a regulator of puberty. *N Engl J Med* **349:** 1614-1627.

Stafford LJ, Xia C, Ma W, Cai Y, and Liu M (2002) Identification and characterization of mouse metastasis-suppressor KiSS1 and its G-protein-coupled receptor. *Cancer Res* **62:** 5399-5404.

Steinberg M (2009) Degarelix: a gonadotropin-releasing hormone antagonist for the management of prostate cancer. *Clin Ther* **31 Pt 2:** 2312-2331.

Takeyama M, Ishida T, Kokubu N, Komada F, Iwakawa S, Okumura K, and Hori R (1991) Enhanced bioavailability of subcutaneously injected insulin by pretreatment with ointment containing protease inhibitors. *Pharm Res* **8:** 60-64.

Tanayama S, Kobayashi T, and Kanai Y (1978) Metabolism of 3-(2', 4', 5' -triethoxybenzoyl) propionic acid, a new biliary smooth muscle relaxant with choleretic activity. I. Disposition after a single administration in rats and dogs. *Xenobiotica* **8:** 365-375.

Toriseva M and Kahari VM (2009) Proteinases in cutaneous wound healing. *Cell Mol Life Sci* **66:** 203-224.

Figure legends

Figure 1. Chemical structures of TAK-448, its M-I metabolite and the internal standard, T-1532583.

Figure 2. Time-profiles for the plasma concentrations of TAK-448 after subcutaneous administration of TAK-448 to rats. TAK-448 was dorsally injected to male SD rats at doses of 0.1 (open circle), 1 (open square) and 10 (open triangle) mg/kg. Each point and vertical bar represents the mean ± standard deviation of five animals.

Figure 3. Time-profiles for the plasma concentrations of TAK-448 after intravenous administration of TAK-448 to rats. TAK-448 was injected into the femoral vein of male SD rats at doses of 0.01 (open circle), 0.1 (open square), 1 (open triangle) and 10 (open diamond) mg/kg. Each point and vertical bar represents the mean standard ± deviation for five animals.

Figure 4. Plasma concentrations of total radioactivity, TAK-448 and M-I after subcutaneous and intravenous administration of [^{14}C]TAK-448 to rats. [^{14}C]TAK-448 was subcutaneously injected at doses of (A) 1 and (B) 10 mg/kg, and intravenously

administered at a dose of (C) 1 mg/kg to male SD rats. Data for the total radioactivity (open circle) represent the mean plasma concentrations for three animals and those for TAK-448 (open square) and M-I (open triangle) represent the concentrations for the pooled plasma from three animals.

Figure 5. Effect of the subcutaneously co-administered protease inhibitor cocktail on the time-profiles for the plasma concentrations of TAK-448 after administration of [^{14}C]TAK-448. [^{14}C]TAK-448 was injected subcutaneously at doses of (A) 1 and (B) 10 mg/kg, and administered intravenously at a dose of (C) 1 mg/kg to male SD rats. Data for the total radioactivity (open circle) represent the mean plasma concentrations for three animals and those for TAK-448 (open square) and M-I (open triangle) represent the concentrations for the pooled plasma from three animals. The subcutaneously administered protease inhibitor cocktail contains 40 mM AEBSF, 20 mM EDTA, 2.6 mM bestatin, 0.28 mM E-64, 0.02 mM leupeptin, and 0.006 mM aprotinin.

Figure 6. Time profile of the metabolism of [^{14}C]TAK-448 in the rat skin homogenate. Skin homogenates (900 μg) prepared from SD rats were incubated at 37°C for 0, 0.5, 1,

2.5, 5, 10, 30 and 60 minutes in the presence of [^{14}C]TAK-448 (1 μg/mL). Each point represents the mean value for two experiments.

Figure 7. Involvement of the metabolic enzymes on the degradation of [^{14}C]TAK-448 in the rat skin homogenate. [^{14}C]TAK-448 (1 μg/mL) was incubated with the rat skin homogenate (900 μg) at 37°C (Control). The concentration-dependency was evaluated in the presence of 100 μg/mL of unlabeled TAK-448. The incubation was carried out at 4°C to estimate the temperature-dependency (ice-chilled conditions). The skin homogenate was pre-heated at 80°C for 15 minutes to inactivate the metabolic activity and metabolism was evaluated as for the control (heat-treated skin). Incubation time was 60 minutes for this experiment. Each column represents the mean ± standard deviation of three experiments.

Figure 8. Effects of the protease inhibitors on the metabolism of [^{14}C]TAK-448 in the rat skin homogenate. [^{14}C]TAK-448 (1 μg/mL) was incubated with the rat skin homogenate (900 μg) at 37°C for 60 minutes with a protease inhibitor cocktail (6 mM AEBSF, 3 mM EDTA·Na, 390 μM bestatin, 43 μM E-64, 3 μM leupeptin and 0.9 μM aprotinin) and with its individual components.

Tables

Table 1 Pharmacokinetic parameters of TAK-448 after subcutaneous and intravenous administration of TAK-448 to rats

Dosing route	Dose (mg/kg)	T_{max} (h)	C_{max} [1)] (ng/mL)	$t_{1/2}$ (h)	AUC [2)] (ng·h/mL)	$V_{d,ss}$ (mL/kg)	CL_{tot} (mL/h/kg)	AUMC/AUC (h)	$MLT_{ab\ site}$ (h)
SC	0.1	0.5 ± 0.0	90.0 ± 12.5	0.5 ± 0.0	123 ± 9	NC	NC	0.971 ± 0.082	0.358
	1	0.9 ± 0.2	381.3 ± 75.5	0.6 ± 0.0	804 ± 133	NC	NC	1.397 ± 0.168	0.797
	10	0.3 ± 0.0	284.6 ± 58.6	0.5 ± 0.0	309 ± 70	NC	NC	0.818 ± 0.071	0.191
IV	0.01	-	24.1 ± 1.2	0.4 ± 0.0	14 ± 1	499 ± 26	770 ± 57	0.650 ±	-

	0.1	-	250.0 ± 17.5	0.4 ± 0.0	140 ± 8	467 ± 28	763 ± 42	0.046 0.613 ± 0.017	-
	1	-	2577.8 ± 240.2	0.5 ± 0.1	1390 ± 155	462 ± 35	774 ± 88	0.600 ± 0.034	-
	10	-	23665.9 ± 3765.8	0.5 ± 0.0	12472 ± 1429	507 ± 51	809 ± 93	0.627 ± 0.010	-

Mean ± S.D. (n=5). -: Not determined. NC: not calculated.

1) C_{max} after IV administration denotes the C_{5min}. 2) 0-24 h.

2) 0-24h.

3) The mean time of loss from the absorption time (MLTab site) after SC administration was calculated by subtracting the AUMC/AUC value after IV administration (i.e., MRT) from the AUMC/AUC value after SC administration at the same dose.

DMD Fast Forward. Published on June 14, 2019 as DOI: 10.1124/dmd.119.087148
This article has not been copyedited and formatted. The final version may differ from this version.

Table 2 Pharmacokinetic parameters of total radioactivity, TAK-448 and M-I in the plasma of rats after subcutaneous and intravenous administration of [^{14}C]TAK-448

Dosing route	Dose (mg/kg)	Component	C_{max} [1)] (μg/mL)	T_{max} (h)	$t_{1/2}$ (h)	AUC (μg·h/mL)
SC	1	Total radioactivity	1.124	1.0	0.6	2.326 (100.0)
		TAK-448	0.624	0.5	0.6	1.184 (50.9)
		M-I	0.396	1.0	0.9	0.712 (30.6)
SC	10	Total radioactivity	6.361	1.0	0.7	16.020 (100.0)
		TAK-448	0.410	0.17	0.7	0.386 (2.4)
		M-I	5.483	1.0	0.9	13.533 (84.5)
IV	1	Total radioactivity	2.990	-	0.5	2.334

				(100.0)
TAK-448	2.693	-	0.5	1.784 (76.4)
M-I	0.122	0.5	0.8	0.196 (8.4)

1) C_{max} of total radioactivity and TAK-448 after IV administration denotes the C_{5min}.

Parameters for total radioactivity are calculated from the mean plasma concentrations for three animals.

Parameters for TAK-448 and M-I are calculated from the concentrations for the pooled samples from three animals. Figures in parentheses denote % of total radioactivity.

Data are taken from Figure 3 and Moriya et al.(2018).

DMD Fast Forward. Published on June 14, 2019 as DOI: 10.1124/dmd.119.087148
This article has not been copyedited and formatted. The final version may differ from this version.

Table 3 Pharmacokinetic parameters of total radioactivity, TAK-448 and M-I in the plasma of rats after co-administration of [^{14}C]TAK-448 and protease inhibitor cocktail

Dosing route	Dose (mg/kg)	Component	C_{max} [1)] (μg/mL)	T_{max} (h)	$t_{1/2}$ (h)	AUC (μg·h/mL)
SC	1	Total radioactivity	0.710	1.0	0.9	1.914 (100.0)
		TAK-448	0.334	1.0	1.0	0.832 (43.5)
		M-I	0.284	1.0	0.9	0.737 (38.5)
SC	10	Total radioactivity	4.739	1.0	1.4	19.103 (100.0)
		TAK-448	1.594	2.0	1.6	5.562 (29.1)
		M-I	2.922	1.0	1.6	10.524 (55.1)
IV	1	Total radioactivity	1.971	-	0.6	2.251

				(100.0)
TAK-448	1.649	-	0.5	1.615 (71.7)
M-I	0.152	0.5	0.9	0.268 (11.9)

2) C_{max} of total radioactivity and TAK-448 after IV administration denotes the C_{5min}.

Parameters for total radioactivity are calculated from the mean plasma concentrations for three animals.

Parameters for TAK-448 and M-I are calculated from the concentrations for the pooled samples from three animals. Figures in parentheses denote % of total radioactivity. Data are taken from Figure 4.

DMD Fast Forward. Published on June 14, 2019 as DOI: 10.1124/dmd.119.087148
This article has not been copyedited and formatted. The final version may differ from this version.

Figures

Figure 1

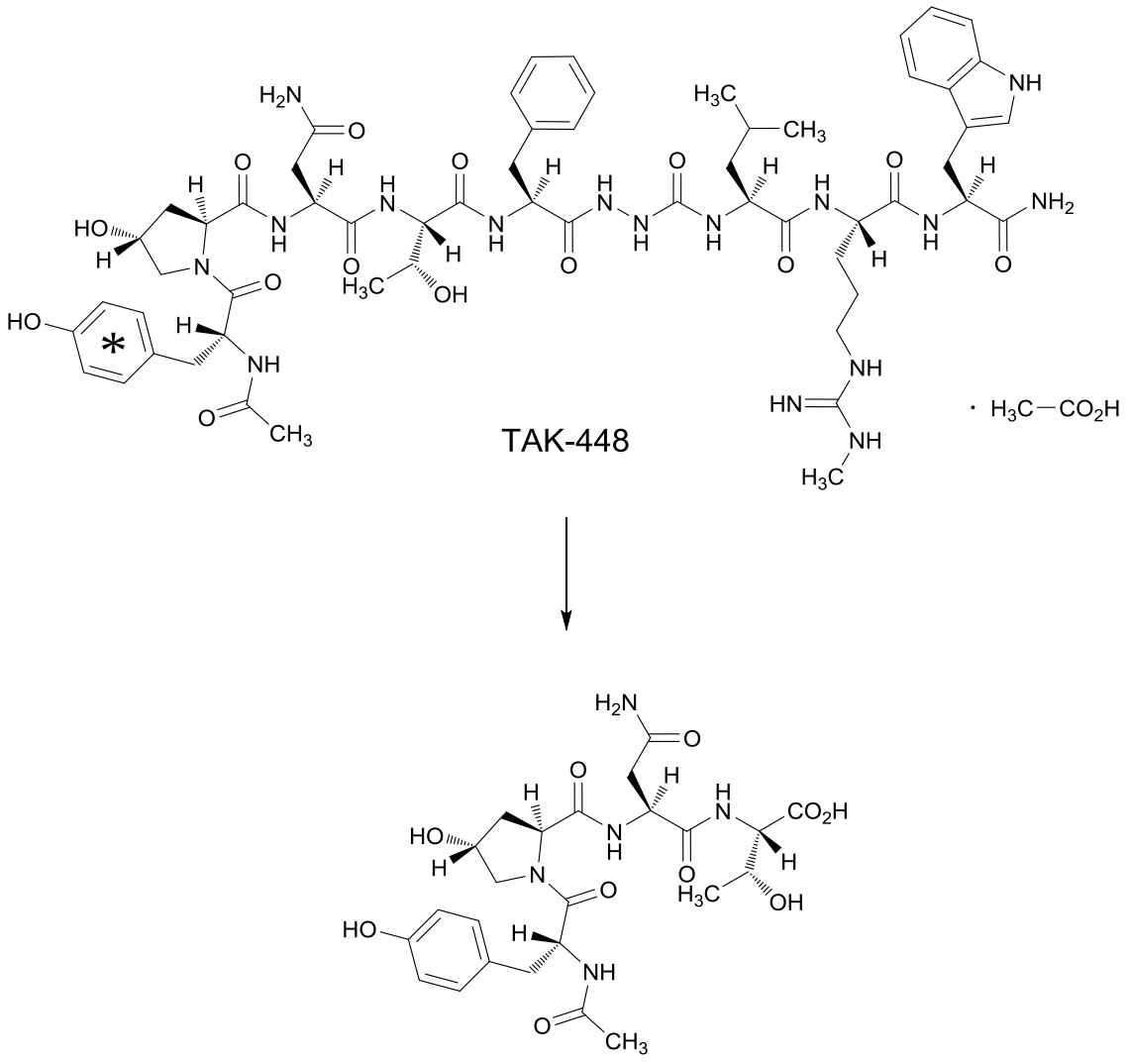

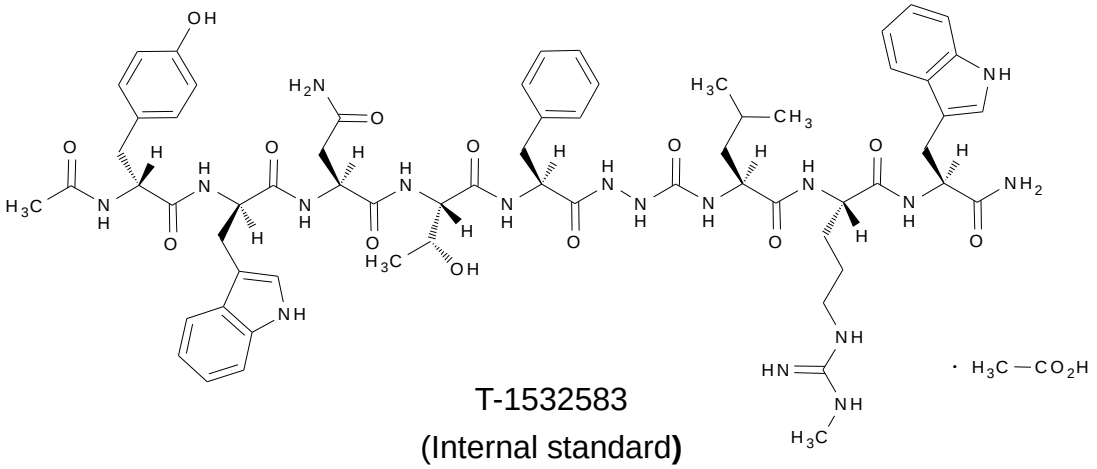

T-1532583

(Internal standard)

DMD Fast Forward. Published on June 14, 2019 as DOI: 10.1124/dmd.119.087148
This article has not been copyedited and formatted. The final version may differ from this version.

Figure 2

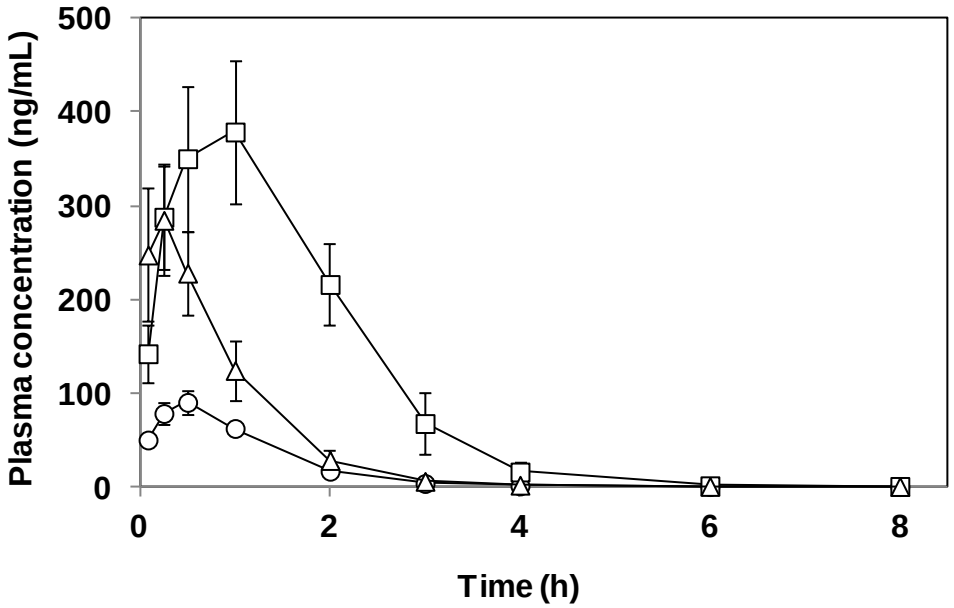

DMD Fast Forward. Published on June 14, 2019 as DOI: 10.1124/dmd.119.087148
This article has not been copyedited and formatted. The final version may differ from this version.

Figure 3

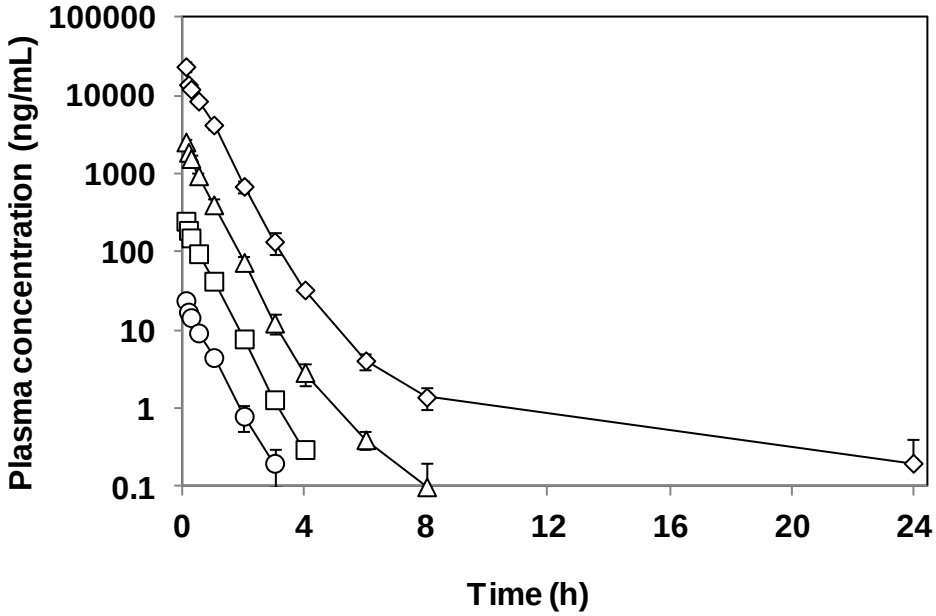

DMD Fast Forward. Published on June 14, 2019 as DOI: 10.1124/dmd.119.087148
This article has not been copyedited and formatted. The final version may differ from this version.

Figure 4

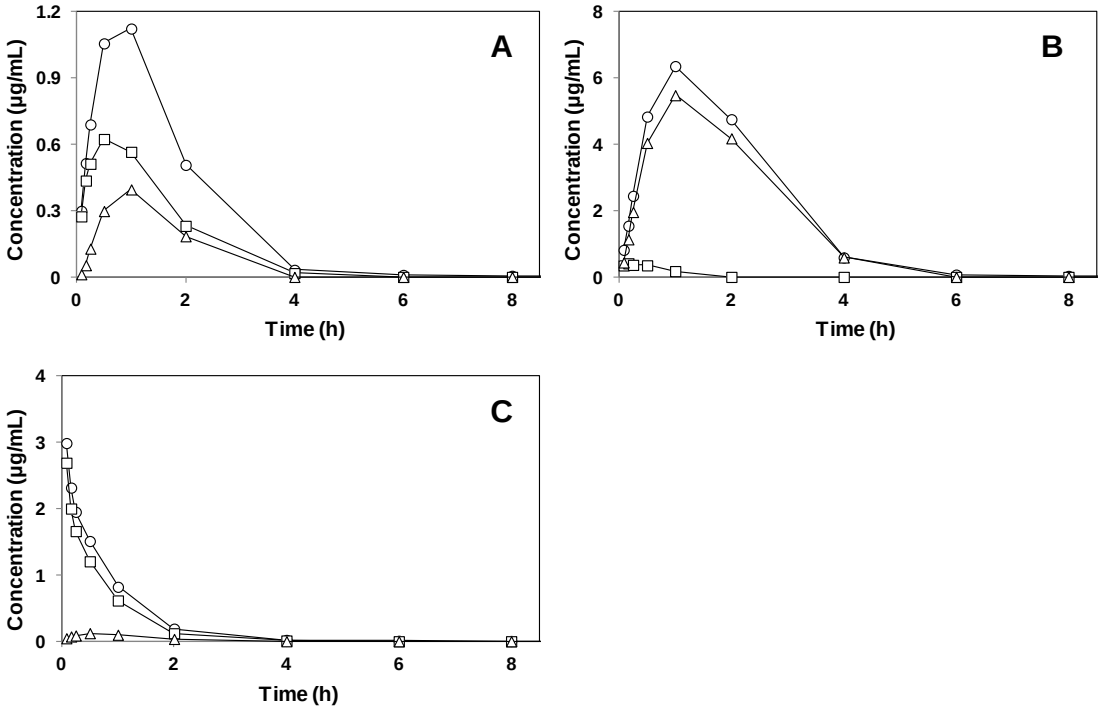

DMD Fast Forward. Published on June 14, 2019 as DOI: 10.1124/dmd.119.087148
This article has not been copyedited and formatted. The final version may differ from this version.

Figure 5

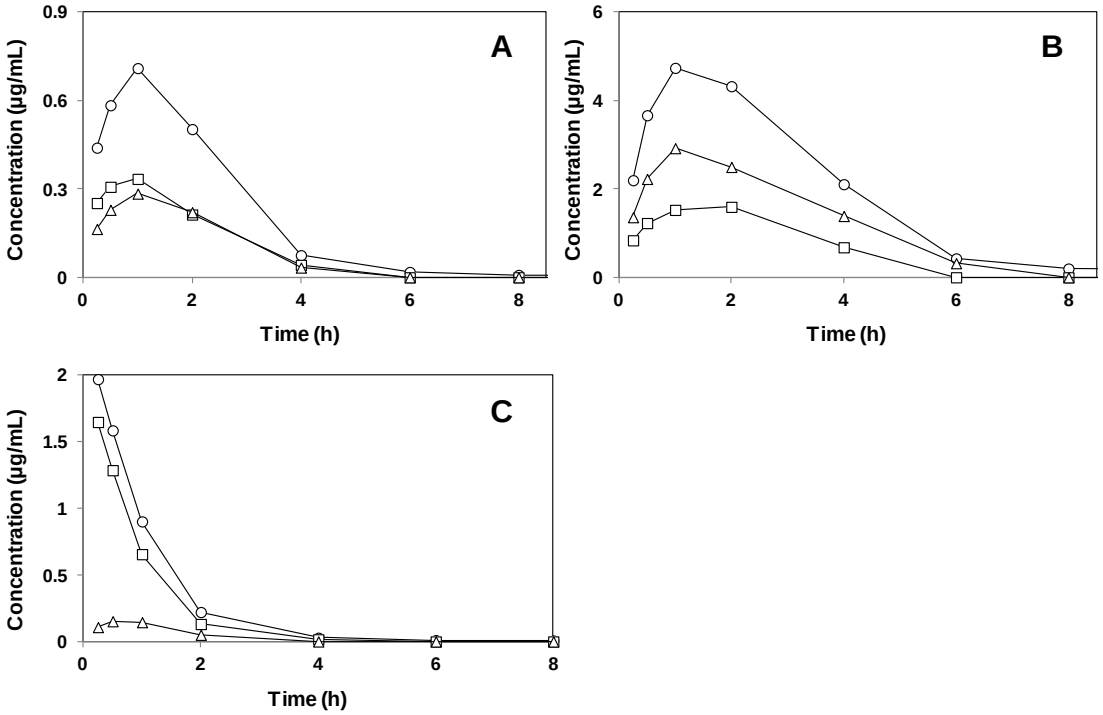

DMD Fast Forward. Published on June 14, 2019 as DOI: 10.1124/dmd.119.087148
This article has not been copyedited and formatted. The final version may differ from this version.

Figure 6

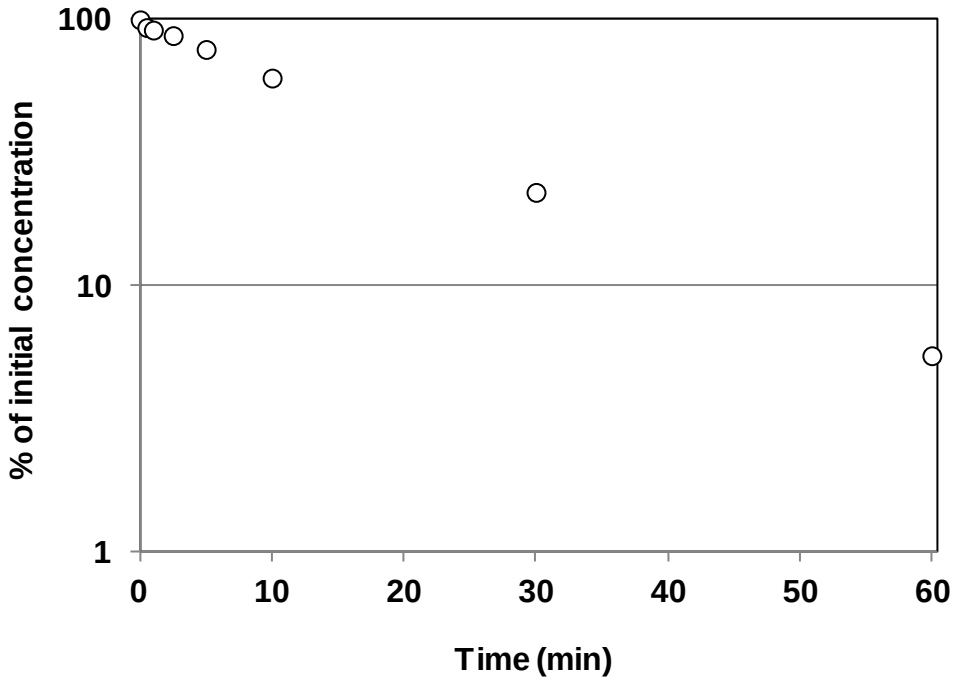

DMD Fast Forward. Published on June 14, 2019 as DOI: 10.1124/dmd.119.087148
This article has not been copyedited and formatted. The final version may differ from this version.

Figure 7

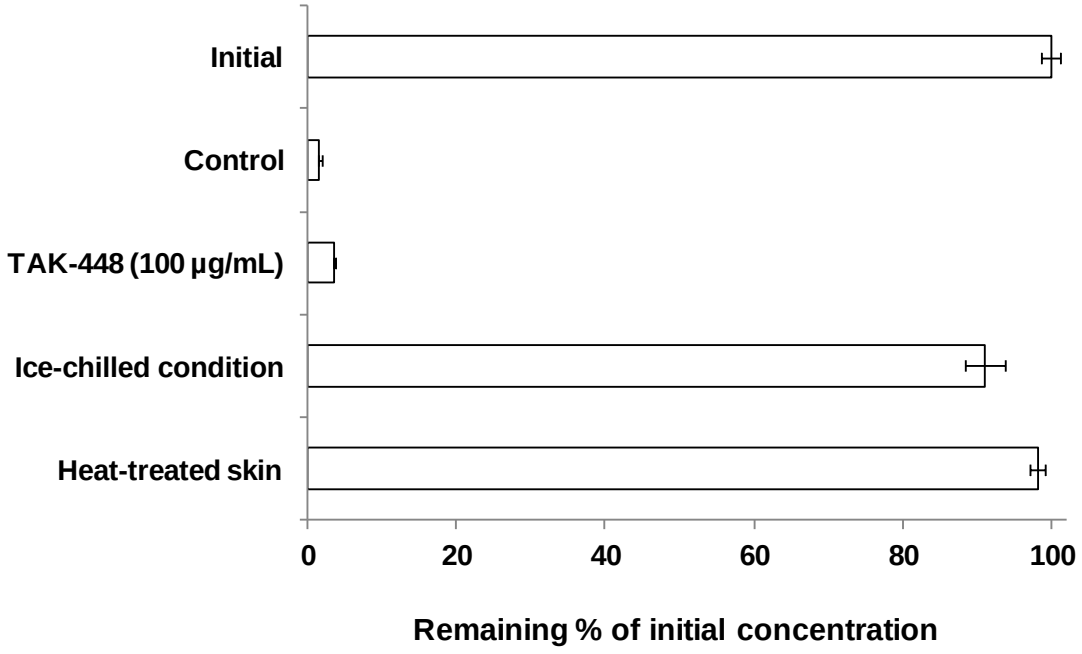

DMD Fast Forward. Published on June 14, 2019 as DOI: 10.1124/dmd.119.087148
This article has not been copyedited and formatted. The final version may differ from this version.

Figure 8

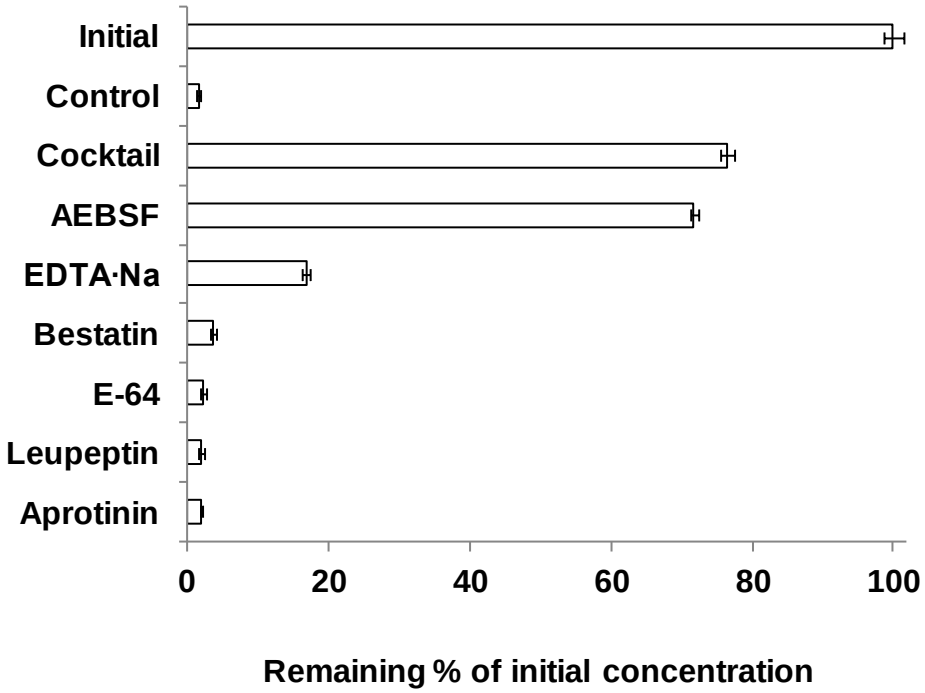

Title:

The enhancement of subcutaneous first-pass metabolism causes non-linear pharmacokinetics of TAK-448 after a single subcutaneous administration to rats

Authors:

Yuu Moriya, Akifumi Kogame, Yoshihiko Tagawa, Akio Morohashi, Takahiro Kondo, Satoru Asahi, Leslie Z. Benet.

Journal title:

Drug Metabolism and Disposition

Supplemental data

Supplemental Table 1 Pharmacokinetic parameters of TAK-448 after subcutaneous and intravenous administration of TAK-448 to dogs

Dosing route	Dose (mg/kg)	T_{max} (h)	C_{max} [1)] (ng/mL)	AUC [2)] (ng·h/mL)
SC	0.1	0.8 ± 0.3	86.6 ± 19.0	252 ± 34
	1	0.8 ± 0.3	882.7 ± 251.3	2596 ± 219
	10	1.0 ± 0.0	8842.5 ± 1202.1	28626 ± 1814
IV	1	-	4254.4 ± 543.4	3093 ± 80

Mean ± S.D. (n=4). -: Not determined.

1) C_{max} after IV administration denotes the C_{5min}.

2) 0-24h.

Supplemental Table 2 Pharmacokinetic parameters of TAK-448 after subcutaneous and intravenous administration of TAK-448 to monkeys

Dosing route	Dose (mg/kg)	T_{max} (h)	C_{max} [1)] (ng/mL)	AUC [2)] (ng·h/mL)
SC	0.1	0.4 ± 0.1	122.6 ± 27.3	295 ± 27
	1	0.3 ± 0.0	1323.4 ± 316.1	2791 ± 262
	10	0.4 ± 0.1	12089.6 ± 2370.2	31576 ± 1396
IV	1	-	5027.0 ± 786.7	3160 ± 594

Mean ± S.D. (n=4). -: Not determined.

1) C_{max} after IV administration denotes the C_{5min}.

2) 0-24h.